UCRL-JC-152017

LAWRENCE
LIVERMORE
NATIONAL
LABORATORY

Raman Generated Magnetic Fields in Laser Light Speckles

B.F. Lasinski, C.H. Still, A.B. Langdon, D.E. Hinkel, E.A. Williams

September 2, 2003

2003 Third International Conference on Inertial Fusion Sciences and Applications, Monterey, CA, September 7-12, 2003

This work was performed under the auspices of the U.S. Department of Energy by University of California, Lawrence Livermore National Laboratory under Contract W-7405-Eng-48.

WP03.38

RAMAN GENERATED MAGNETIC FIELDS IN LASER LIGHT SPECKLES.

Barbara F. Lasinski, Charles H. Still, A. Bruce. Langdon,
Denise E. Hinkel, and Edward A. Williams

Lawrence Livermore National Laboratory
Box 808, Livermore CA 94551

lasinski1@llnl.gov

In modern 2D and 3D PIC simulations relevant to National Ignition Facility (NIF) parameters, the low frequency magnetic fields associated with the localized fast electron currents generated by Stimulated Raman Scatter have been identified. We consider electron plasma densities from 0.1 to 0.2 of critical density (n_c) and electron plasma temperatures (T_e) from a few keV to over 10 keV in simulations with space scales corresponding to a laser speckle in modeling with our massively parallel PIC code Z3. These magnetic fields are ~ 1 MG. Then the electrons accelerated by the Raman process are magnetized with their Larmor radii on the order of a speckle width. The transport of these hot electrons out of the speckle then becomes a more complex process than generally assumed.

I. INTRODUCTION

Particle-in-Cell (PIC) codes provide a fully kinetic, nonlinear plasma description and are a key tool for studying laser-plasma interactions in high energy density applications. Here we describe modern PIC simulations of Stimulated Raman Scatter (SRS) in which the high intensity incident laser scatters off the electron plasma waves of the underdense plasma. The aim of these PIC studies is to elucidate the SRS saturation mechanisms with a view to mitigating the associated energy loss. A recent reference on SRS in PIC codes is Langdon and Hinkel[1] in which the rescatter of the scattered light was identified as a saturation mechanism. Further work on Raman saturation in PIC simulations is also being presented at this conference.[2]

We are primarily concerned with the expected conditions of laser-plasma interactions in hohlraums to be irradiated at the National Ignition Facility (NIF). There will be 192 f/20 beams arrayed in 48 quads, each described by f/8 optics. At the target, the high-power laser light consists of "speckles" of about equal size and distributed exponentially in intensity. The fraction of power with laser intensity $I > I_0$ is $\sim (1 + I/I_0)\exp(-I/I_0)$, where I_0 is the average laser intensity. Therefore ~4% of the incident laser power has intensities greater than $5I_0$. The speckle size is length ~ SRS, as well as other laser plasma interaction physics, occurs most strongly in the more intense of these speckles. Here we consider average laser intensities greater than 10^{15} W/cm^2 for 351 nm (blue) laser light. Plasma densities range from 0.1 – 0.2 n_c, where n_c is the critical density, the density at which the laser frequency w_0 equals the plasma frequency ω_{pe}. Electron plasma temperatures range from 5 to 14 keV, depending on the hohlraum size.

In laser light speckles, SRS, independent of the direction of the scattered light, generates localized currents of forward going electrons. These currents result in surrounding magnetic fields, which have been identified for the first time in our simulations. We find that for vigorous SRS these magnetic fields are roughly 1 MG and are large enough to inhibit the lateral transport of both the background electrons and the Raman generated hot electrons. Thus, the magnetic fields have an impact on electron transport in these plasmas and on SRS saturation,

In Section II, we describe our PIC modeling. SRS in these modern PIC simulations is described in Section III and these results are discussed in Section IV.

II. Z3

Both large PIC simulations and dedicated diagnostics are the key ingredients in obtaining these new results. PIC codes used in modeling SRS include Ampere-Faraday-Maxwell fields, relativistic particle dynamics, and particle-in-cell coupling of particles to fields. Our code, **Z3**, is a modern rewrite of **ZOHAR**, our serial, 2D (two spatial dimensions for particles and fields) code described in reference 3. **Z3** includes the third spatial dimension and is designed to exploit modern massively parallel computers. Now, the larger PIC simulation volumes and longer time scales are much closer to actual experimental conditions. Simulating an entire f/8 speckle in 3D is now feasible. With **Z3** on 512 processors, we have modeled an f/4 speckle as a capability demonstration. That simulation volume was 2510 x 2510 x $153\lambda_0$ and contained 7.6 x 10^9 particles. This achievement allows direct comparison with single-speckle experiments and more macroscopic simulations.

As part of the diagnostic suite, we apply a low pass temporal filter, $[\sin(\pi\omega/\omega_0)/(\pi\omega/\omega_0)]^2$, over two laser periods to fields and fluxes to separate the laser and the lower frequency fields and fluxes. We identify the filtered quantities with the subscript s.

The **Z3** simulation geometry has z as the laser propagation direction and x and y as the transverse dimensions. Boundary conditions are "open" in z and periodic in x and y. Particles that reach the z-boundaries are absorbed. The laser spatial profile is either Gaussian or $(\sin)^4$. Temporally the laser has a short rise time of xx ps and then remains flat.

III. Z3 SIMULATIONS OF STIMULATED RAMAN SCATTER

We model in 3D an incident laser at 7 x 10^{16} W/cm^2 for 351 nm light interacting with a flat plasma density profile at 0.2 n_c at 14 keV. These parameters correspond to an intense speckle in a small hohlraum irradiation. In this simulation the laser is linearly polarized in the (B_x, E_y) plane and is incident at z = 0.

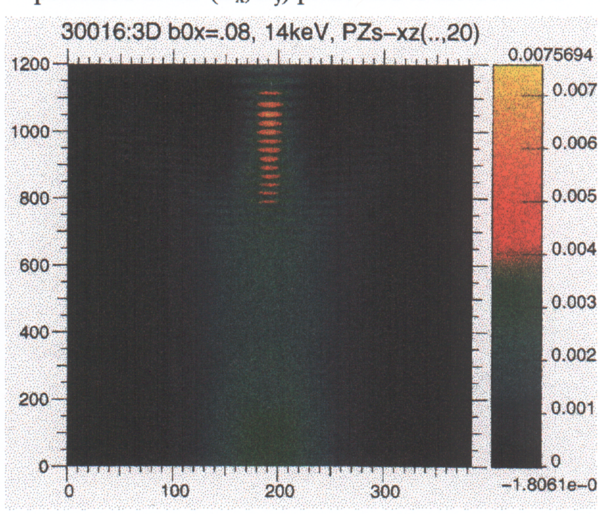

Fig. 1 is a plot of the filtered Poynting flux, (Pz)s in the Ly/2 plane versus x and z at 0.27 ps.

We expect to find vigorous forward and backward Raman scatter at these parameters. In Fig. 1, we plot the low frequency component of the Poynting flux, $(P_z)_s$ in the central $L_y/2$ plane at 0.27 ps. The longer wavelengths associated with Raman back and forward scatter are separately distinguishable.

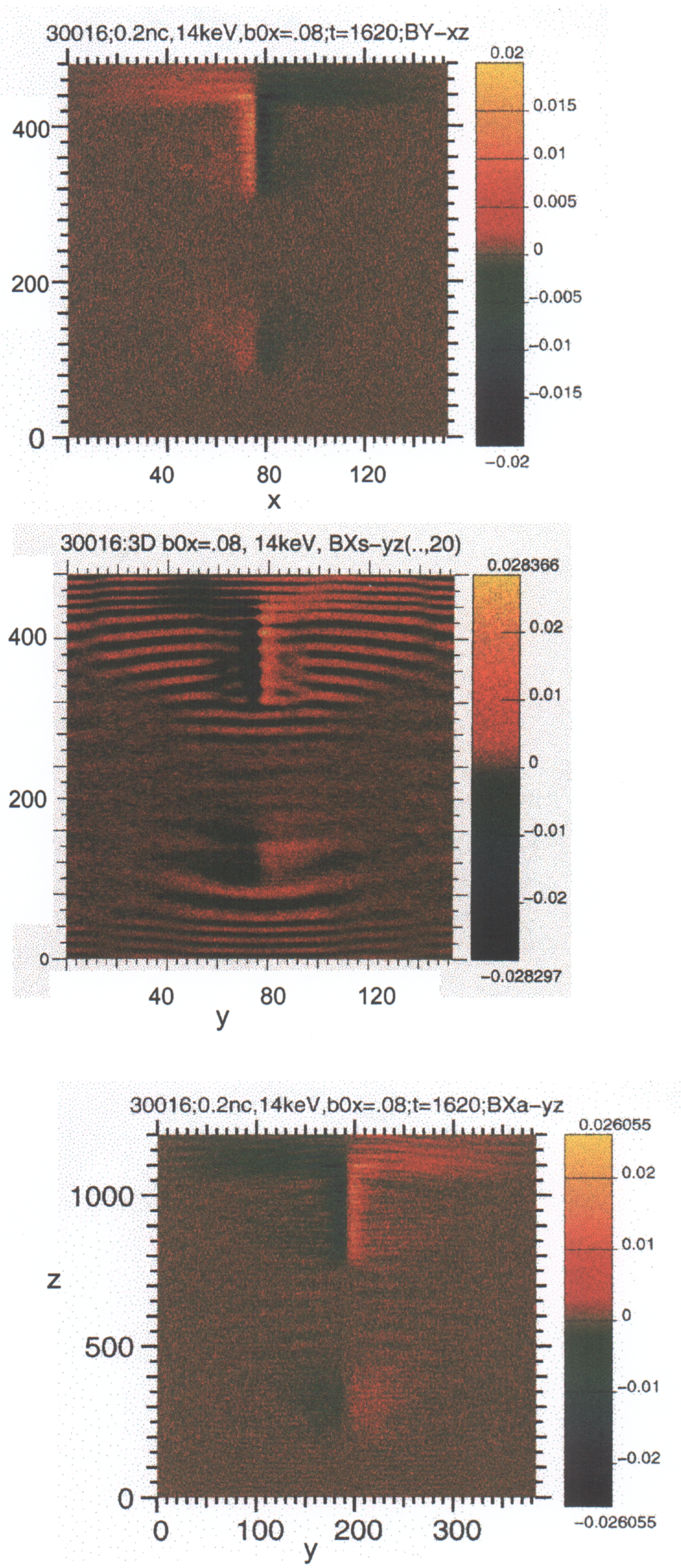

Fig. 2 shows a) B_y vs x and z at $L_y/2$, b) filtered B_x vs y and z at $L_x/2$, and c) the antisymmetic component of the field shown in b. All these plots are at 0.27 ps in the 3D simulation.

At the same time in the simulation, the static magnetic fields associated with back and forward scatter are shown in Fig. 2a. We plot B_y, the component of B without the incident laser, vs (x, z) in the $L_y/2$ plane. Large magnetic fields are evident in the regions of forward and back SRS. In these units, B = 0.02 corresponds to 6 MG.

Raman back and forward scatter, as well as their associated magnetic fields, are readily visible in the 2D slice of $(B_x)_s$, Fig. 2b. Here the low-pass filtering on the component of the magnetic field containing the pump field removes the incident laser. The filtered array then shows both the static magnetic field and the long wavelengths of Raman back and forward scatter. The antisymmetric component of $(B_x)_s$, plotted in Fig. 2c, involves further filtering and isolates the static magnetic field.

By comparing Figs 2a and 2c, we find the B_x and B_y components of B_{theta} which are consistent with a net negative current, J_z. That is, the static magnetic field is consistent with a current of forward-going electrons, as is produced by SRS.

The Larmor radius of electrons in a magnetic field greater than 1 MG is smaller than an f/8 speckle width. Here, the peak magnetic field at 0.27 ps is 6 MG. Then an 80 keV hot electron has a Larmor radius of ~ $3\lambda_0$, which is less than a speckle width and in rough agreement with the narrow spatial extent of B_{theta} observed in the simulations. We then infer that the net current associated with this magnetic field is on the order of an Alfven current.

We also have done 2D simulations with these same parameters. In 2D, we can readily simulate bigger systems for longer times. In a 2D simulation which is the length of an f/8 speckle, 512 λ_0, and which was run past 1 ps, there is significant SRS before the laser has traversed the entire speckle, as shown in Fig. 3. We find the expected bursts of SRS. At 0.4 ps in this simulation, before the laser reaches the back of the speckle, we find the filtered magnetic field similar in magnitude to those shown in Fig. 2b and 2c. In this 2D geometry, with the pump linearly polarized such that its electric field is in the simulation plane, that is the only component of the static magnetic field, B_{theta}, that can occur.

We find weaker versions of these static magnetic fields when Raman scatter is less vigorous. With the same geometry as in the simulation described for Fig. 2, we have done another 3D simulation of Raman scatter in a plasma at 0.2 n_c , Te = 5 keV, irradiated by an incident laser at intensity 1.5 x 10^{16} W/cm^2 (blue). Here, at 0.31 ps, we find a filtered magnetic field at peak value ~0.5 MG. This field is still strong enough to inhibit transverse flow of 20 keV hot electrons out of the instability region of an f/8 speckle.

At a lower density, 0.15 n_c, we also find bursts of Raman back and forward scatter in a 2D simulation which is 290 λ_0 long. Here Te = 5 keV and the incident laser in again 1.5 x 10^{16} W/cm^2 (blue). This simulation was also continued past 1 ps. At this lower density SRS is less vigorous and at 0.98 ps, we find a weak filtered magnetic field of ~ 0.06 MG. Here, it is not obvious what role, if any, this weak magnetic field has in saturating SRS.

IV. SUMMARY

In 3D and large 2D PIC simulations, we have, for the first time, identified the low frequency magnetic fields generated by the currents of fast electrons associated with SRS. We have shown that these fields are large enough to confine the heated particles to the instability region with a laser light speckle. Thus, these magnetic fields affect instability saturation and electron transport in the underdense plasma.

ACKNOWLEDGMENTS

This work was performed under the auspices of the U.S. Department of Energy by University of California Lawrence Livermore National Laboratory under contract No. W-7405-Eng-48.

REFERENCES

1. A. B. Langdon and D. E. Hinkel, Phys Rev Lett **89**, 15003-1 (2002).
2. Denise Hinkel *et al*, paper TuO7.5, this meeting and A. Bruce Langdon *et al*, paper WP03.35, this meeting.
3. C. K. Birdsall and A. B. Langdon, *Plasma Physics via Computer Simulation* (McGraw-Hill, New York, 1985).

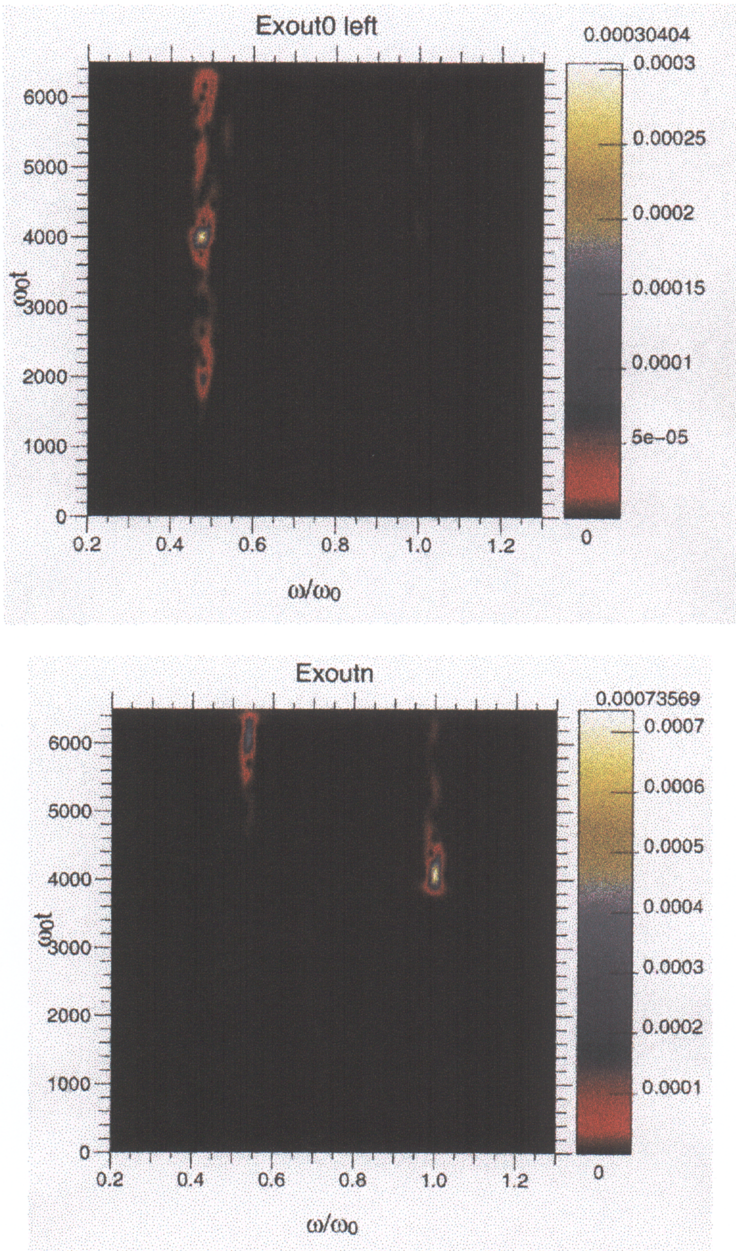

Fig. 3 shows the frequency of the input and out light as a function of time in the 2D simulation at 0.2 n_c, 14 keV, 7 x 10^{16} W/cm^2. In a) we see the backscattered light which is dominated by Raman backscatter at ~0.5 ω_0. In b) we see the slightly higher frequency of Raman forward scatter. Frequencies are relative to ω_0 and times are such that 6000 = 1 ps.